Biochemical and Biophysical Research Communications **272,** 55–63 (2000)
doi:10.1006/bbrc.2000.2742, available online at http://www.idealibrary.com on IDEAL®

Dynamic Measurement of Single Protein's Mechanical Properties

Keita Mitsui,*,† Ken Nakajima,† Hideo Arakawa,* Masahiko Hara,† and Atsushi Ikai*,[1]

**Faculty of Bioscience and Biotechnology, Tokyo Institute of Technology, Nagatsuta, Midoriku, Yokohama, Kanagawa, 226-8501, Japan; and †Frontier Research System, RIKEN, Hirosawa, Wako, Saitama, 351-0198, Japan*

Received April 19, 2000

Dimerized (tandemly repeated) protein was constructed, and the stretching force during the unfolding of the single protein molecule was measured using an atomic force microscope. In quasistatic measurements using normal force–distance curve measurements, each monomer unit was unfolded step by step. To elucidate the conformational state at each extension length, we measured the relax–stress response of the protein using short stroke sinusoidal movements of the sample stage. This allowed us to investigate the dynamic response of the protein repeatedly without full stretching or rupturing. Although the protein molecule responded in-phase to the applied movement in most cases, we found a novel out-of-phase response around the stretching length where the second monomer unit unfolded. Applying the spring constant measured in the quasistatic experiment, the out-of-phase response was reproduced in the simple calculation, which suggested the folding and the unfolding at the second monomer unit were taking place repeatedly during the relax–stress response measurement.

A scanning probe microscope (1) (SPM) has been used not only for observation but also for nanoscopic characterization, in which the microscope is a tool to detect several kinds of physical or chemical properties from local regions. Several macroscopic parameters, such as electronic conductance (2), permittivity (3), magnetic properties (4), elasticity (5) and viscosity (6) have been measured on a nanoscopic level. Measuring all these parameters on single molecules might be one ultimate goal (7, 8) of nanoscopic characterization by SPM.

This study was conducted because of the importance of a more in-depth understanding of the unfolding and folding phenomena of proteins in the field of bioscience. The process of protein folding and unfolding has been studied on a large population of protein molecules so far (9). The ensemble of native, denatured and intermediate states was measured as an average of these several condensed states. At intermediate states, those which were constructed with one intermediate or several intermediates or a mixture of native and denatured protein were indistinguishable. Considering that several pathways may exist between the folding state and unfolding states and that each molecule may choose different pathways because there are several local minima and several unfolding states, it is necessary to examine a single molecule to understand the details of the folding–unfolding process.

Recently, a direct approach technique to intramolecular force has been achieved using optical tweezers (10) and an atomic force microscope (AFM) on giant protein (11, 12). An experiment on a polymer sample (13) that can be considered as a model for denatured protein has been already performed.

To study the intramolecular force by AFM, a methodology for attaching a molecule between a substrate and an AFM tip is required. One successful method that we recently reported (12) utilizes chemisorption between Au and thiol. An atomically flat and stable Au (111) surface, an Au coated AFM tip and the protein into which the thiol groups were introduced using a bioengineering technique are needed for well-controlled studies of intramolecular force (14). In our previous report, we compared the difference between the methods of introducing thiols on the protein randomly and intentionally. Well-controlled studies were done, but it was still unclear whether the protein was folded at each extended length. We proposed that the final condition was perhaps a random coil.

Herein we report systematic AFM studies of intramolecular force for a dimerized bovine carbonic anhydrase B (CAB) molecule. The following points are suitable for immobilization and precise handling of our measurement. The structure of human CAB has been determined by X-ray crystallography. N- and

[1] To whom correspondence should be addressed. Fax: 81-45-924-5806. E-mail: aikai@bio.titech.ac.jp.

0006-291X/00 $35.00

C-terminal exist near both poles of this globular protein, and these terminals are the easiest sites to introduce cysteine residues. We assumed that the structure of bovine enzyme is similar to human CAB. The sequence of bovine CAB contains no cysteine residues originally, however, the introduced cysteine residues become the handling points through Au-S bonds. Using the dimerized protein allows us to expand protein two times longer than the original monomer protein and to analyze the sample as two similar serially connected structures. The dimerized CAB was mechanically unfolded by stretching using an AFM tip in a highly reproducible way. The required force for unfolding each monomer unit was coincidental in order with the folding energy of CAB which has been reported elsewhere (15).

Dynamic measurements as well as quasi-static measurements are required to study mechanical properties, especially for polymers, because polymers intrinsically have viscoelastic properties that only can be investigated by dynamic measurements. This approach will clarify the difference between simple random-coil polymers and proteins that have high order structures, such as α-helix and β-sheet. We proposed in this paper one technique for a nano-viscoelastic measurement equipped with AFM. This equipment is realized by applying sinusoidal excitation needed to measure the sample protein in the same manner as a macroscopic viscoelastic measurement for polymers.

EXPERIMENTAL

Protein production and purification. In this study, we constructed dimer CAB. Dimer CAB sequence is based on the wild-type bovine CAB, and the connection between the two monomer units was formed through 4 amino acid residues (Glu-Phe-Lys-Lys), and at each terminal, cysteine residues were added. The dimer cDNA sequence was then obtained. Protein production and purification were carried out using an Xpress System (Invitrogen, Carlsbad, CA). One hundred mM DTT was added to the stock solution to avoid crosslinking between molecules through disulfide bonds. The protein solution was passed through a short column of Sephadex G-25 (Pharmacia, Uppsala, Sweden) or HPLC column of TSK-GEL G3000SW (TOSOH, Tokyo, Japan) to remove DTT. The mutated sequence and the complete coding region were checked by plasmid sequencing.

Substrate and tip. Au (111) substrates on mica for AFM measurement were prepared as previously described (16). The mica was cleaved in the atmosphere, and a thin film of gold around 100 nm in thickness was deposited on the mica at 400°C (substrate heater temperature) at 10^{-6} Pa. The Au coated tips were obtained from Olympus (TR400-PB-1, Tokyo, Japan).

Sample preparation. The protein solutions were diluted to 40 μg/ml, and 20 μl of the solution was cast on Au (111)/mica substrate. After 5 min incubation, the surface was rinsed with a buffer solution (50 mM Tris–SO_4, pH 7.5).

Quasistatic force measurement. Force–distance curve measurements were taken with a NanoScope III multimode microscope (Digital Instruments, Santa Barbara, CA) equipped with a fluid cell. The force–distance curve was taken in a way that the cantilever approached and finally touched the sample and then was retracted to the initial position without lateral scanning. The force detected on the cantilever was calculated from the cantilever deflection with the cantilever spring constant (0.02 N/m). During the approach and retraction, the cantilever deflection reflects various kinds of repulsive and attractive forces exerted from the sample to the tip. We focused on the sample deformation recorded during the retraction in the force curve measurement. If the sample was expanded during the retraction, the sample stage position and the position of the cantilever deflection differed by the extension length of the sample. From this result we obtained the "force extension curve." All measurements were performed in 50 mM Tris–H_2SO_4 buffer solution at pH 7.5. The typical scan range and the scan rate of the force–distance curve measurement were 250 nm and 0.03 Hz, respectively.

Dynamic measurement. We newly constructed an AFM piezo controller together with special software for a dynamic nano-rheological measurement. It allowed us to design any required movement of the sample stage in the z direction, especially for the sinusoidal movement which is used in macroscopic rheological studies. We measured the sample's dynamic responses through recording both the cantilever deflection and the piezo movement, which showed the response of the protein and the applied modulation, respectively. In the event of usual random coil spring, the response of the cantilever against the applied modulation shows the in-phase responses.

Enzyme assay. The esterase activity of CAB was measured with *p*-nitrophenylacetate (*p*NPA) (17) as substrate for the esterase. CAB reacts with pNPA and produces *p*-nitrophenol (*p*NP) whose concentration was detected by absorbance at 348 nm. All measurements were done with 1 mM *p*NPA and 50 mM phosphate buffer solution at pH 7.5 in the cell of a spectrometer. The purified protein solutions were prepared in the cell and then *p*NPA was added. For protein activity on the Au (111)/mica substrate, we prepared the sample as follows: Au (111)/mica substrate was placed in the cell parallel to the light path so as not to interrupt the light path of the source and the detector. One hundred micro-liters of a 40 μg/ml sample solution was applied to Au (111)/mica substrate to cover a 9 mm $\times$ 9 mm area, and incubated for 5 min. The surface was then rinsed with buffer solution.

RESULTS

The molecular density on the substrate was crucial in order to sandwich a single molecule between the AFM tip and the substrate. We believe that we detected the single mechanical unfolding process because of the following reasons. First, the chance of detecting significantly large forces reflecting the picking up a protein molecule was one out of 60 during a series of trials. Most of the remaining curves showed only a slight adhesion force of less than 5 pN. With such limitations, it was difficult to anticipate where two or more molecules were expanded at the same time. Curves with a slight extension of the sample with a strong adhesion were also detected in approximately one out of one thousand cases, but we did not consider these cases as a single molecular event. Second, the fact that the final extension length corresponding to linear length of CAB suggested that we measured the extension of a single protein.

The typical curves obtained in these experiments are shown in Fig. 1. Three major peaks were observed. During the extension, two small force peaks were first observed and finally a third large force peak was ob-

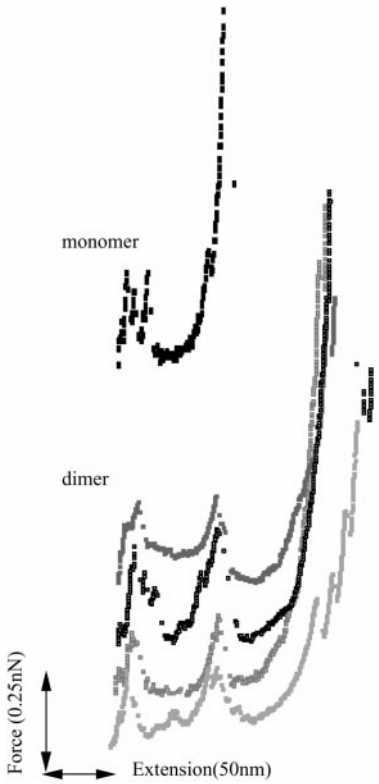

FIG. 1. Quasistatic force extension curves of single dimerized protein molecules. Some force extension curves of dimerized protein from a number of the experiments are shown together with an example of monomer protein for comparison. Force–distance curves were measured and converted to force–extension curves as described in the text. Dimerized protein showed a characteristic middle peak at the extension where monomer protein was pulled near its full extension with the similar force.

served. In the case of the monomer protein as shown in the upper part of Fig. 1, we could not observe the second small force peak. Finally, the molecule extended to around 100 nm. The distribution of extension lengths at the middle peak and final peak is summarized in Fig. 2. For a case with no sample extension, the cantilever deflection follows the z piezo movement exactly until the sample is detached from the tip. If the sample extension was carried out, the cantilever deflection changed to a z piezo movement minus sample extension length. Thus, the zero point of the extension is assigned to the point where the sample deformation starts. This histogram clearly shows that the extension length at the middle peak (73 $\pm$ 14 nm) was about half of that at the final peak (155 $\pm$ 21 nm). This suggests that after the first monomer unit in the dimer was unfolded, just as in the case of the monomer protein, the second monomer unit was unfolded by the force at the middle peak. The comparison between the previous and present results implies that the first two peaks correspond to the unfolding processes, and the last peak corresponds to the full extension of the polypeptide chain.

Figure 3 shows the distribution of the forces applied at the first peak and the middle peak. The similarity of both forces at the first and second peaks suggests that the same phenomena occurred, and each of the two monomer units unfolded under each peak. As shown in Fig. 1, after the first peak and the middle peak, the protein molecule was extended largely with a small applied force. Thus the peaks at 0.1 nN on Fig. 3 suggest that this force may be the threshold of the catastrophic phase change of the protein conformation, where a three-dimensional folded structure changes to a random-coil structure.

The protein activities on the gold surface are summarized in Table 1. The amount of protein on the surface was calculated to be about 0.22 μg, assuming one protein occupies the area of 25 nm^2 and the protein layer forms full coverage. Although we measured a certain threshold in the detected forces during the stretch, the activity of the dimer on the gold substrate was quite low. We concluded that the proteins on the surface lost their activity but were not totally denatured, and still had some structures. We will discuss the denaturation possibility later.

Dynamic response measurement was performed at several extension lengths of a single dimerized protein. At each extension point, 4 cycles of sinusoidal modulation were applied to the piezoelectric that moved the substrate (0.25 Hz, peak to peak amplitude fixed at 40 nm). Figure 4 shows several different behaviors of the cantilever responses against the sinusoidal input. When the tip touched the surface, the response followed the input signal (Fig. 4a). In Fig. 4b, where the tip was not touching the surface but pulled by a sandwiched molecule (this situation was observed in almost same ratio on a static measurement), the cantilever

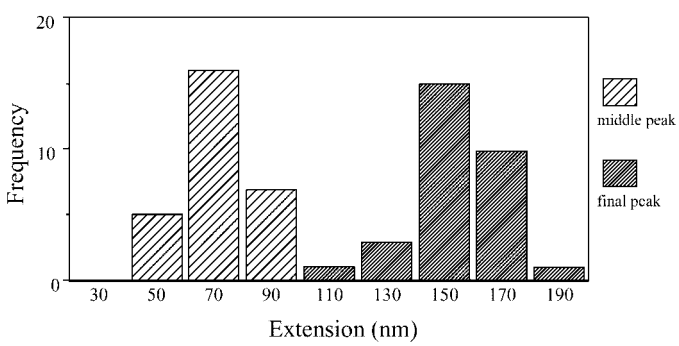

FIG. 2. Distributions of the extension length of the dimerized protein at the middle peak and at the rupture. A histogram was made from 30 force–extension curves of which two showed no middle peak. The two distributions were clearly separated and both showed regular distribution around their average. The average value of the full extension length (155 nm) was about double that of the middle peak (73 nm), which is coincident with the model that one domain of the dimerized protein was unfolded at the first peak and the other domain was broken at the middle peak. Details are discussed in the text.

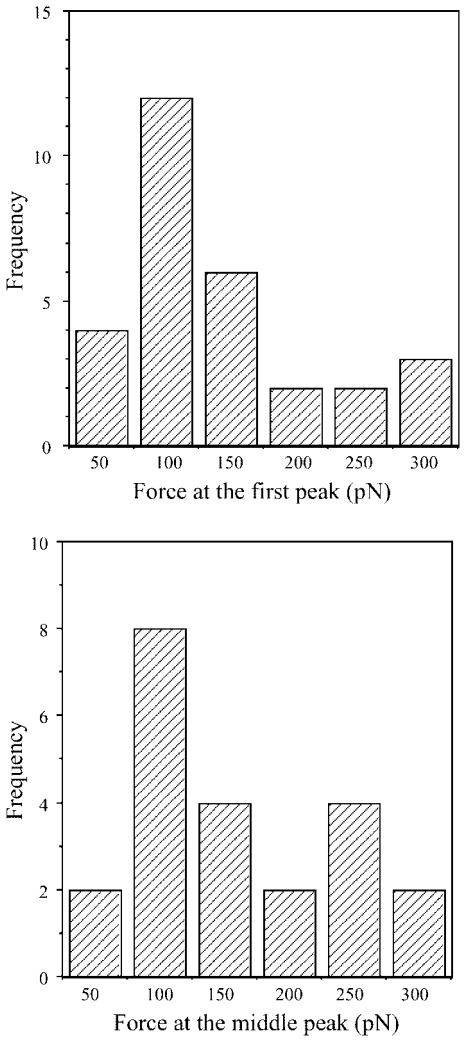

FIG. 3. Distributions of the forces applied at the first peak and the middle peak. The histogram of the force at the first peak (a) and at the middle peak (b) showed quite similar distributions around 100 *p*N. This suggests that similar events were taking place in the two peaks, possibly the unfolding of each domain.

showed small movements that were in-phase to the applied modulation. The molecule was sometimes detached from the tip during the modulation, as shown in Fig. 4c. In the same displacement between the substrate and the tip without the sandwiched molecule, there was no response against the modulation as shown in Fig. 4d. These results show that the response like b is not caused by the viscosity of the liquid between the cantilever and the substrate surface. At a certain extension length, the molecular response against an applied stress became out-of-phase (Fig. 4d) (about half of the responses were the out-of-phase responses), which is an extraordinary behavior from macroscopic rheological consideration. To elucidate the phenomenon in detail, we investigated the changes between in-phase and out-of-phase molecular response signals which depended on extension length as shown in Fig. 5. The estimation of the exact extension length was difficult because the recalculation needs to take the exact instrument drift into account during the experiment (mainly the thermal and electrical effects). In the long extension range the possibility of the tip becoming detached from the molecule increases. The out-of-phase response was observed at an estimated range of 40 nm to 100 nm.

DISCUSSION

From the quasi-static extension experiment the following phenomena on the protein stretching event can be suggested. It is necessary to consider that the protein is immobilized almost directly on the gold surface, which causes some changes in the native protein (e.g., increasing adhesion or denaturing). To investigate the changes in conditions of the protein from the solid-like state to the random-coil-like state, we performed the dynamic measurement.

In the quasistatic extension experiment, compared with previously reported data on monomer stretching (14), the final extension length was about two times longer than that for the monomer. The extended length after the middle peak was a slight longer than that before the middle peak, because the force applied at the rupture event was much larger than the force at the middle peak. The length at the middle point extension of the dimer was almost the same as that for the monomer. In summary, Figs. 2 and 3 suggest that the dimerized CAB was extended in a stepwise fashion when the threshold forces were applied. Assuming the two tandem parts of this protein as the same two springs, each spring jointed in a serial way should be straightened at the same time, however, in this measurement each part of this protein was expanded individually. We then consider that the threshold force causes the phase transition of protein from the folded structure to the random-coil-like structure at each tandem part. At the first peak of the force extension curve, the monomer unit that has the weaker threshold force becomes the random-coil-like structure, and the other

TABLE 1

Activity of Seveal Condition of CAB *p*NPA Is Self Decay to *p*NP, Real Activity Was Calculated from Blank Reference

Sample	Rate of *p*NP production (mM/min)	Activity
blank	0.541	—
native CAB (0.22 mg/ml)	1.020	0.479 (100%)
blank with gold substrate	0.643	—
dimer (0.22 mg/ml)	0.850	0.309 (64.5%)
dimer on gold substrate	0.744	0.101 (21.1%)

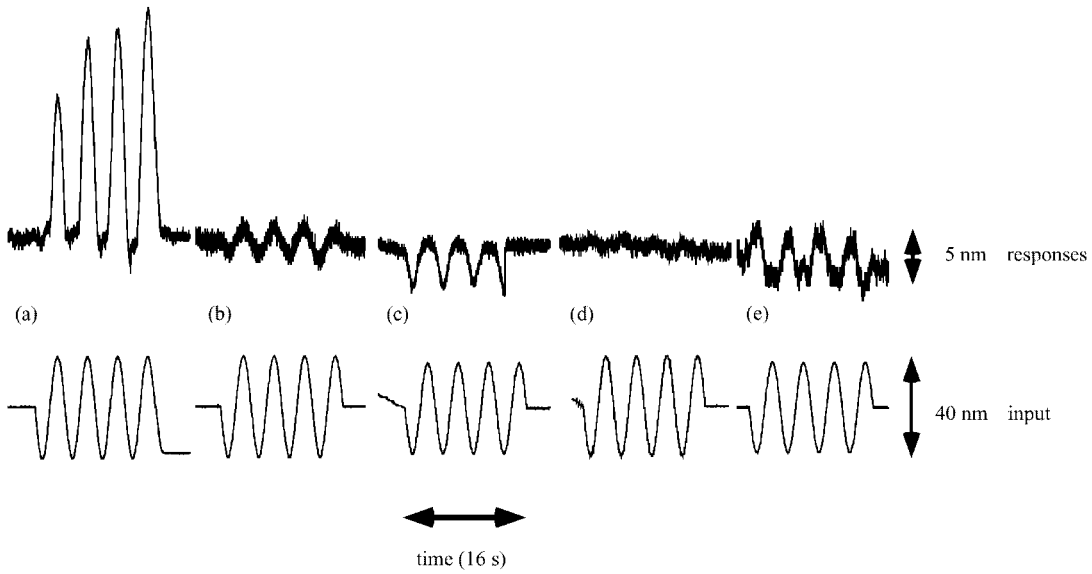

FIG. 4. Examples of dynamic nanorheological measurement. (a) When the tip cyclically touched the surface, the cantilever was pushed up while the tip was in contact. (b) The in-phase response was observed occasionally. The amplitude was quite different from that of (a). (c) The in-phase response sometimes disappeared during the oscillation. The protein may be detached at the forth modulation in this case. (d) No response was observed even when the distance from the substrate was the same as in the case of (b), if the sample was not sandwiched. (e) Out-of-phase response, which could not happen if the sample had behaved as a simple spring was also observed.

monomer unit remains as the folded structure until the next threshold force is applied. Two assumptions about the difference of the threshold force can be considered. First, one monomer unit that is attached directly on the substrate is partially denatured because it stays on a bare metal surface. This partial denaturation makes the threshold force weaker. Second, the conformation of each monomer unit slightly perturbed thermally, and these slight differences in conformations cause the difference of threshold forces at each expanding event.

There is the possibility that properties of the denatured protein were measured, which was also suggested from the enzyme assay, because the protein stayed on hard metal substrate, and during force measurement the force was loaded on the protein, which might cause the protein to denature. However, from Fig. 3 the forces of the first peak and middle peak were almost the same, which suggests both monomer units kept almost the same stability. It was a very rare case for the protein to be expanded without a middle peak, which also suggests that the protein on the surface still remained in some folded state. Even if the protein was partially denatured, we think that the denatured level is quite low. First, the effect of the loading force did not cause serious damage to the sample, which was shown in the reproducibility of these data. Second, the observed low activity of the enzyme can be explained by assuming that the surface was not fully covered. The expected amount of the protein was low. To estimate the real coverage on the surface, a molecular resolving AFM image or surface plasmon resonance spectroscopy, etc., is necessary. Third, the consumed energy at the second peak of the force curve (Fig. 1), that is calculated to be around 50 kcal/mol from the peak area, is not so far from the value of ensemble–average experiment, where the energy for the folded–unfolded transition is calculated from the stability of CAB (ΔG = 10.8 kcal/mol) by the guanidation (15) experiment. The difference between the values can be interpreted as follows. The estimated energy here includes not only the enthalpic contribution due to the transition but also the enthropic one. In other words, the decrease of the entropy of the other monomer unit during the extension might be also added to the consumed energy, because one monomer unit that had been already disentangled after the first peak can act as random coil and show the enthropic elasticily. The rate of denaturation was still unknown, but the result in the quasi-static measurement supports the drastic change of the protein conformation during the extension.

In the dynamic measurement, the accurate position of the substrate surface was not clear because of the drifts of the piezoelectrics. We could know the exact position only when the tip surface touched the substrate surface, though the position during noncontact (connected only through the protein molecule) movement was important to obtain the position dependency of the response. Therefore the exact position of the surface was estimated from those data that shows the touching of the tip directly by the substrate as shown in Fig. 4a, by interpolation. Then the following results were obtained. The in-phase responses of the protein molecule are measured in the distance ranges from II to III and from IV to V (Fig. 5, inset), suggesting the

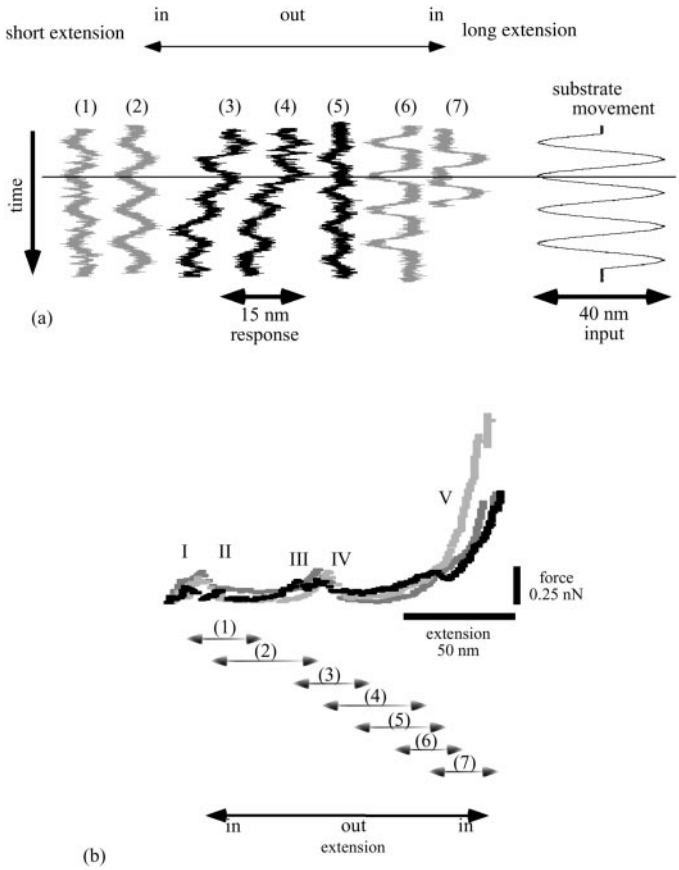

FIG. 5. (a) The distance dependence of the cantilever response. The cantilever responses are aligned according to the length of the extension. The out-of-phase responses, (3–5), were observed in a certain region of the extension, while the in-phase responses, (1, 2, 6, and 7), were observed in shorter or longer extensions. (b) The relation between the quasi-static experiment data and the positions of the extension where the responses shown in (a) were observed.

nature of the random coil dominates these regions. On the other hand, the out-of-phase responses were measured in the range from III to IV, which can not be explained by any macroscopic rheological consideration. It only gives at most 90 degree phase shift for the perfect viscous fluid and never results in 180 degree shift. It is also difficult to explain the phenomena in terms of any kinds of resonance, such as the cantilever (10 ~ 100 kHz) and the measurement system (0.1 ~ 10 kHz), since the modulation frequency used in the experiment is quite slow (0.25 Hz). In order to peruse the possible interpretation, we constructed a simple models described below. We treat the present AFM system (cantilever, sample and stage) as a serially connected spring and the one end of which is moving according to the sinusoidal signal (Fig. 6a). The input signal was applied as

$$X_2 = A \sin \omega t, \qquad [1]$$

where A is the amplitude of the modulation and ω is the modulation angular frequency. The equation of motion becomes as

$$m_c \ddot{X}_1 = -k_c X_1 + k_p (X_2 - X_1), \qquad [2]$$

where m_c is the effective mass of the cantilever and k_c is the spring constant of the cantilever and k_p is the

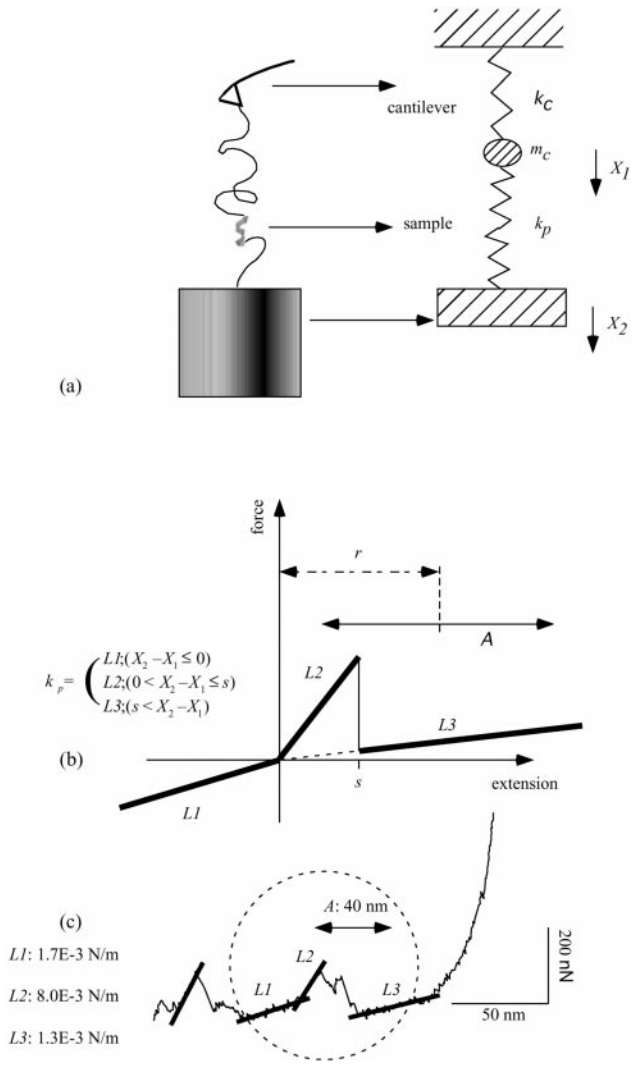

FIG. 6. (a) The relation between the simulation model and the experimental setup. X_1 (response) and X_2 (input) are displacements of the cantilever and the stage, respectively. m_c is effective mass of this model and k_c and k_p are the spring constants of the cantilever and the sample, respectively. (b) The model for the sample spring constant shown in force–extension curve. Spring constants are shown as slopes of each linear line. According to extension length, the spring constant changes $L1$, $L2$, to $L3$. A and r are the amplitude of the modulation and the center of that modulation, respectively. Each parameter was taken from the quasistatic result and the dynamic measurement ($A = 20$, $\omega = 1.74$, $m_c = 0.001$, $k_c = 20$, $L1 = 1$, $L2 = 10$, $L3 = 0.5$, $s = 10$). (c) An example of corresponding real quasistatic datum.

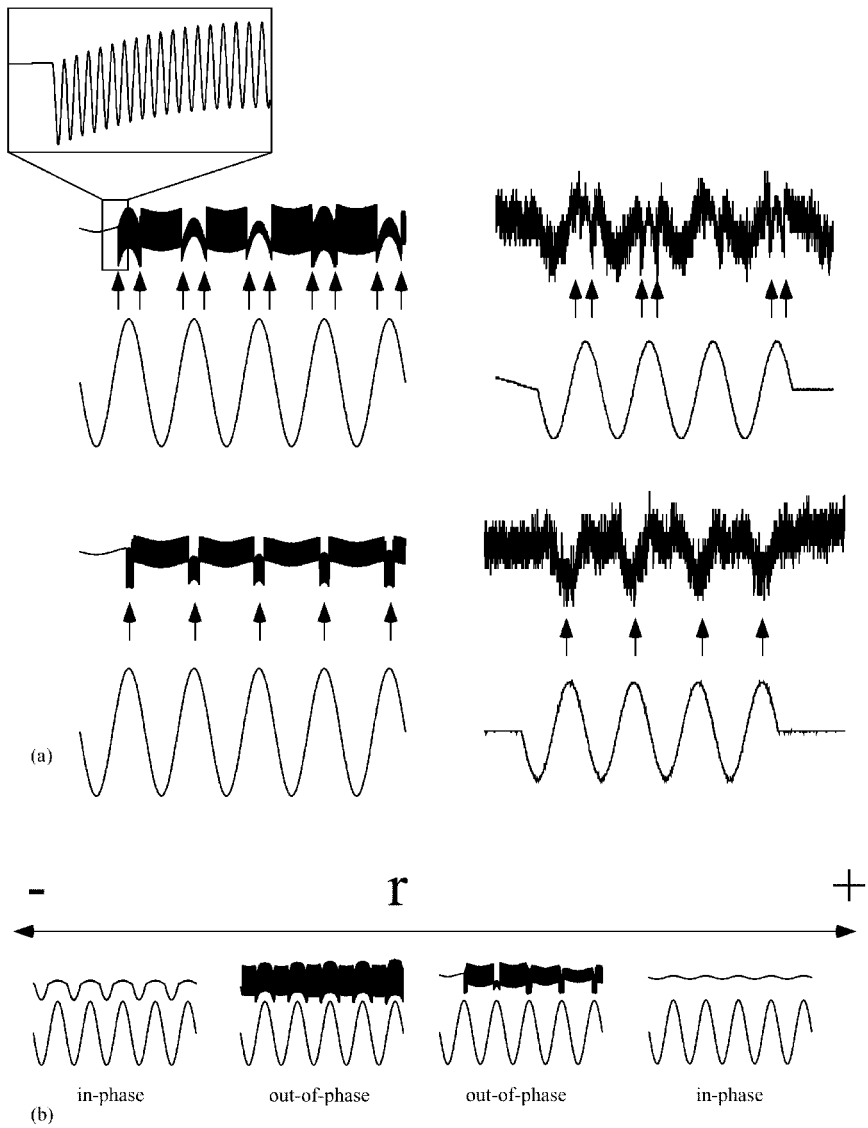

FIG. 7. (a) Some characteristic shapes of the response are reproduced, as indicated by the arrows. The results of simulation and measurement are shown in left and right, respectively. A part of the simulation is enlarged to show that the high frequency oscillation overlapped the signal. This high frequency oscillation will be dumped when the viscosity of solvent is applied in calculation. Each parameter was taken from Fig. 6 with r as 20 and 29. (b) The results of the simulation arranged along r. The responses changed from in-phase to out-of-phase and then back to in-phase again according to the increase of r, which corresponds to Fig. 5a.

spring constant of the sample. The main part of this model was that we introduced a nonlinear spring with three spring constants as the sample spring. Thus the sample spring constant was discontinuously changed at the distance s. This shape of the spring constant was constructed according to a quasistatic measurement (Fig. 6b), resulting in a sudden formation of some local structures if the distance between the appropriate residues reaches below a certain threshold (simulation parameter: s). This local structure strengthens the spring constant as the natural rubber becomes strong by vulcanization. For example, α-helix and small protein can fold within 20 μs (18), and from the CD signal the secondary structure of CAB is restored completely within less than 15 s (19). The model shape originally came from the shape in the ranges from III to IV, which is related to the second monomer unit unfolding. The simulation reproduced the shape of the response and the distance dependence in the same order of each parameter (e.g. sample spring constant, applied modulation, etc.). This simulation shows a similar response shape (Fig. 7a). Some parts of the simulated shape did not yet reproduce the exact shape as the out-of-phase response because we did not include any viscostic parameter that is usually included in a rheology simulation, which will smooth the step-like change of the shape (Fig. 7a). The extension length dependence is shown in Fig. 7b as changing the initial condition of the

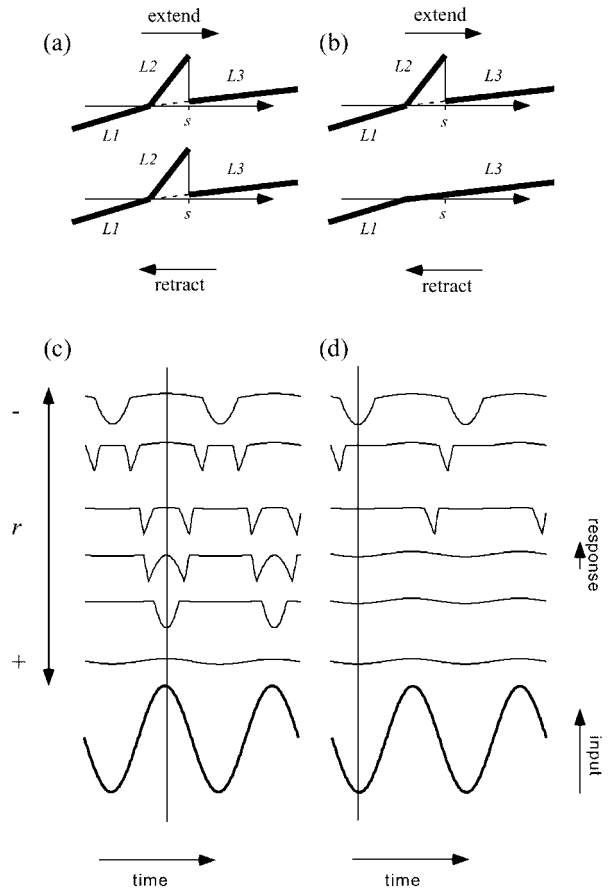

FIG. 8. Spring constants shown in force–extension curves without hysteresis (a) and with hysteresis (b). The spring constant $L2$ is not reproduced during retraction in hysteresis model. $X1$ positions (the responses) calculated from the equilibrium of forces are shown in (c) and (d) for nonhysteresis and hysteresis model, respectively. The out-of-phase responses similar to Fig. 7a were reproduced in the nonhysteresis model, while the hysteresis model produced only some phase shifted responses. The result strongly suggests that the spring constant $L2$ (or the middle peak) in the retraction is necessary for the out-of-phase responses.

extension (simulation parameter: r). From this dependence, the edge of the amplitude of the modulation needs to be very near the threshold point. When the amplitude of the modulation does not overlap the threshold, the response is jumped in the out-of-phase shape. We also calculated the X_1 position just from the equilibrium of the forces and added the hysteresis of the sample spring constant that is difficult to introduce to a simulation algorithm (Fig. 8). The hysteresis means that the protein did not generate the force for folding during the retraction (20). Figure 8 shows that the nonlinearity at the retraction is important to reproduce the out-of-phase response. This is the first report of observing the force generated during a folding event as far as we know.

We should consider the possibility that these frequency behaviors could have been caused by water dumping, while from Figs. 4c and 4d we conclude this phenomena was observed only when the molecule was attached between the substrate and the tip, and in this frequency range the water dumping effect is not high enough to be observed.

We have to understand why only the dynamic measurement showed the refolding event where a short stroke sinusoidal scan was used, while the quasistatic measurement gave no force during the retraction process. Comparison with the recent famous report for the much larger protein (titin) may reveal a certain guideline (20). There the force during the unfolding event was repeatedly observed in a similar quasistatic measurement when a long duration after the retraction was set between the trial. Nevertheless, even in this case, no force was observed in the retracting process. In both quasistatic measurements, molecules were extended over the several monomer units (>200 nm, the number of tandem repeats of titin and our protein were eight and two repeats, respectively), that may lead to a misfolding also as described in the titin paper. The stroke length of 40 nm in the dynamic measurement was at least 4 times shorter, where the parts of the molecule may almost keep their own configurations after the unfolding. Thus, it is much easier to refold again during the retracting loop. The scan velocity might be an important factor because, as described in the titin paper, we may not observe the refolding event if the scan rate is too high. However, the scan velocities of the titin case and our quasistatic measurement were 400–600 nm/s and 15 nm/s, respectively. On the other hand, that of our dynamic measurement was 20 nm/s. The former two conditions did not result in the refolding during the retraction, but the last did in spite that the velocity was in between.

Another approach to the folding event is the modulation frequency dependence. The comparison of frequency response especially in much lower frequencies with the polymer which will reproduce the in-phase phenomena on this system will reveal more details of denatured protein, and the part of the drastic conformational changing may also depend on the frequency of the modulation. These experiments are in progress.

CONCLUSION

These investigations open significant areas of research with AFM for the future. For example, basic folding–unfolding information for a single molecule that will be relevant to chemists and biologists can be extracted from these studies. A well-controlled applied force on a single molecule could lead to new rheology field. This may lead a new field of nanorheology with the AFM system.

REFERENCES

1. Bottomley, L. A. (1998) *Anal. Chem*. **70,** 425R–475R.
2. Jiang, C.-S., Nakayama, T., and Aono, M. (1999) *Appl. Phys. Lett.* **74,** 1716–1718.
3. Franke, K., Huelz, H., and Weihnacht, M. (1998) *Surf. Sci.* **415,** 178–182.
4. Skidmore, G. D., and Dahlberg E. D. (1997) *Appl. Phys. Lett.* **71,** 3293–3295.
5. Stroup, E. W., Pungor, A., and Hlady, V. (1996) *Ultramicroscopy* **66,** 237–249.
6. Radmacher, M., Fritz, M., Kacher, C. M., Cleveland, J. P., and Hansma, P. K. (1996) *Biophys J.* **70,** 556–567.
7. Xie, X. S. (1996) *Acc. Chem. Res.* **29,** 598–606.
8. Ha, T., Ting, A. Y., Liang, J., Caldwell, W. B., Deniz, A. A., Chemla, D. S., Schultz, P. G., and Weiss, S. (1999) *Proc. Natl. Acad. Sci. USA* **96,** 893–898.
9. Cleland, J. L., and Wang, D. I. (1990) *Biochemistry* **29,** 11072–11078.
10. Trombitas, K., Greaser, M., Labeit, S., Jin, J. P., Kellermayer, M., Helmes, M., and Granzier, H. (1998) *J. Cell Biol.* **140,** 853–859.
11. Rief, M., Gautel, M., Oesterhelt, F., Fernandez, J. M., and Gaub, H. E. (1997) *Science* **276,** 1109–1112.
12. Mitsui, K., Hara, M., and Ikai, A. (1996) *FEBS Lett.* **385,** 29–33.
13. Nakajima, K., Yamaguchi, H., Lee, J. C., Kageshima, M., Ikehara, T., and Nishi, T. (1997) *Jpn. J. Appl. Phys.* **36,** 3850–3854.
14. Ikai, A., Mitsui, K., Furutani, Y., and Hara, M. (1997) *Jpn. J. Appl. Phys.* **36,** 3887–3893.
15. Cupo, P., El-Deiry, W., Whitney, P. L., and Awad, W. M., Jr (1980) *J. Biol. Chem*. **255,** 10828–10833.
16. Nishida, N., Hara, M., Sasabe, H., and Knoll, W. J. (1997) *Jpn. J. Appl. Phys.* **36,** 2379–2385.
17. Pocker, Y., and Stone, J. T. (1967) *Biochemistry* **6,** 668–678.
18. Duan, Y., and Kollman, P. A. (1998) *Science* **282,** 740–744.
19. Kern, G., Kern, D., Schmid, F. X., and Fischer, G. (1995) *J. Biol. Chem*. **270,** 740–745.
20. Oberhauser, A. F., Marszalek, P. E., C-Vazquez, M., and Fernandez, M. (1999) *Nat. Struct. Biol.* **6,** 1025–1028.